Fourier Analysis of Clamped Moderately Thick Arbitrarily Laminated Plates

Reaz A. Chaudhuri* and Humayun R. H. Kabir†
University of Utah, Salt Lake City, Utah 84112

Nomenclature

A_{ij}, B_{ij}, D_{ij} = extensional, (bending-stretching) coupling, and bending rigidities, respectively
a, b = dimensions of the plate parallel to the x_1 and x_2 axes, respectively
E_i = Young's modulus in the x_i direction
G_{ij} = shear modulus in the i-j plane ($i \neq j$)
h = total thickness of a laminated plate
K = shear correction factor
m, n = modal wave numbers in x_1 and x_2 directions, respectively
N_i, M_i = in-plane stress resultants and stress couples, respectively
q = distributed transverse load
u_i = components of displacement at the reference surface (x_1, x_2, 0) in x_i direction
x_i = orthogonal Cartesian coordinates
ν_{12} = major Poisson's ratio in the x_1-x_2 plane
ϕ_i = rotation of the normal to the reference surface

Introduction

THE single most important factor to commercial and military aircraft designers alike is the design flexibility inherent in the fiber reinforced composite laminates, known as tailoring, which is essentially exploiting the possibility of obtaining optimum design to meet specific design requirements. Derivation of analytical solutions for these laminates, even for the simplest kind of geometry, e.g., rectangular plates, is, however, fraught with many complexities, such as in-plane anisotropy, asymmetry of lamination (resulting in bending-stretching coupling), transverse shear deformation (due to low transverse shearing stiffness to longitudinal stiffness ratio), etc. Additional complexities arise by way of satisfying boundary conditions, e. g., all edges clamped, that cannot be handled by traditional analytical approaches, such as almost two centuries-old Navier's and close to a century-old Levy's . The primary objective of the present study is to derive a boundary-continuous-displacement solution, using a recently published generalized Navier's approach,[1,2] to the problem of static response of an arbitrarily laminated plate, involving five highly coupled second-order-linear partial differential equations (PDEs), together with the rigidly clamped boundary conditions prescribed at all four edges. Numerical results presented include 1) convergence characteristics of the deflection and moment, 2) study of the effect of thickness, and 3) variation of displacements and moments along the length of the laminated plate.

Problem Statement and Solution Methodology

The governing system of five PDEs in terms of the reference surface displacements and rotations is obtained in accordance with the first-order shear deformation theory (FSDT) or Yang-Norris-Stavsky (YNS) theory,[3] which takes into account the effect of transverse shear deformation in a manner suggested by Mindlin. In the interest of brevity of presentation, only the first three are shown as follows:

$$\begin{aligned} &G(i,\,1)u_{1,11} + G(i,\,2)u_{1,12} + G(i,\,3)u_{1,22} + G(i,\,4)u_{2,11} \\ &\quad + G(i,\,5)u_{2,12} + G(i,\,6)u_{2,22} + G(i,\,7)\phi_{1,11} \\ &\quad + G(i,\,8)\phi_{1,12} + G(i,\,9)\phi_{1,22} + G(i,\,10)\phi_{2,11} \\ &\quad + G(i,\,11)\phi_{2,12} + G(i,\,12)\phi_{2,22} = 0; \qquad i = 1,\,2 \end{aligned} \tag{1a}$$

$$\begin{aligned} &G(3,\,1)u_{3,11} + G(3,\,2)u_{3,12} + G(3,\,3)u_{3,22} + G(3,\,4)\phi_{1,1} \\ &\quad + G(3,\,5)\phi_{1,2} + G(3,\,6)\phi_{2,1} + G(3,\,7)\phi_{2,2} = q \end{aligned} \tag{1b}$$

in which

$$\begin{gathered} G(1,\,1) = A_{11}; \quad G(1,\,2) = 2A_{16}; \quad G(1,\,3) = A_{66} \\ G(1,\,4) = A_{16}; \quad G(1,\,5) = A_{12} + A_{66}; \quad G(1,\,6) = A_{26} \\ G(1,\,7) = B_{11}; \quad G(1,\,8) = 2B_{16}; \quad G(1,\,9) = B_{66} \\ G(1,\,10) = B_{16}; \quad G(1,\,11) = B_{12} + B_{66}; \quad G(1,\,12) = B_{26} \\ G(2,\,1) = A_{16}; \quad G(2,\,2) = A_{12} + A_{66}; \quad G(2,\,3) = A_{26} \\ G(2,\,4) = A_{66}; \quad G(2,\,5) = 2A_{26}; \quad G(2,\,6) = A_{22} \\ G(2,\,7) = B_{16}; \quad G(2,\,8) = B_{12} + B_{66}; \quad G(2,\,9) = B_{26} \\ G(2,\,10) = B_{66}; \quad G(2,\,11) = 2B_{26}; \quad G(2,\,12) = B_{22} \\ G(3,\,1) = G(3,\,4) = KA_{55}; \quad G(3,\,2) = 2KA_{45} \\ G(3,\,3) = G(3,\,7) = KA_{44}; \quad G(3,\,5) = G(3,\,6) = KA_{45} \end{gathered} \tag{2}$$

The rigidly clamped boundary condition is prescribed as follows[1,2]:

$$u_i = 0, \;\; i = 1,\,2,\,3 \qquad \phi_i = 0, \;\; i = 1,\,2 \qquad \text{at all edges} \tag{3}$$

The boundary-continuous displacement solution technique, as presented by Chaudhuri[4] and valid for any boundary condition, dictates that the solution for a rigidly clamped plate be assumed, for $x_i \in [0,\,a]\; x[0,\,b]$, $i = 1,\,2$, in the form of a double Fourier sine series, as follows[1,2]:

$$\begin{aligned} (u_1,\,u_2,\,u_3,\,\phi_1,\,\phi_2) &= \sum_{m=1}^{\infty} \sum_{n=1}^{\infty} \\ &\times (U_{mn},\,V_{mn},\,W_{mn},\,X_{mn},\,Y_{mn}) \sin(\alpha x_1) \sin(\beta x_2) \end{aligned} \tag{4}$$

where

$$\alpha = m\pi/a, \qquad \beta = n\pi/b$$

The total number of unknown constant coefficients defined in Eq. (4) are $5mn$. Assumed solution functions (4) completely satisfy the geometric boundary conditions (2) in a manner similar to Navier's approach. Expansion of the transverse load into a double Fourier sine series

$$q = \sum_{m=1}^{\infty} \sum_{n=1}^{\infty} q_{mn} \sin(\alpha x_1) \sin(\beta x_2) \tag{5}$$

and substitution of the assumed functions (4) and their partial derivatives into the governing PDEs (1) will, after a slight rearrangement, supply a set of five linear equations for $x_i \in (0,\,a)\; x(0,\,b)$, $i = 1,\,2$. Direct application of the conventional Navier's method, which involves equating the coefficients of $\sin(\alpha x_1) \sin(\beta x_2)$, $\sin(\alpha x_1) \cos(\beta x_2)$, etc., will yield, in

Received Sept. 30, 1991; revision received April 26, 1992; accepted for publication April 26, 1992.

*Associate Professor, Department of Civil Engineering. Member AIAA.

†Graduate Research Fellow, Department of Civil Engineering; currently, Senior Research Engineer, Engineering Mechanics Research Corporation, Troy, MI 48083.

total, $16mn$ equations in $5mn$ unknowns, thus failing to provide a solution to this physical problem. To overcome this difficulty, the next and more important step is to expand $\cos(\alpha x_1)\cos(\beta x_2)$, $\cos(\alpha x_1)$, and $\cos(\beta x_2)$ in the form of the corresponding Fourier sine series, for $x_i \in (0, a)\, x(0, b)$, $i = 1, 2$, in a manner suggested by Green and Hearmon,[5] as follows:

$$\cos(\alpha x_1)\cos(\beta x_2) = \sum_{r=1}^{\infty}\sum_{s=1}^{\infty} h_{mr}h_{ns}\sin(\gamma x_1)\sin(\Psi x_2) \tag{6a}$$

$$\cos(\alpha x_1) = \sum_{r=1}^{\infty} h_{mr}\sin(\gamma x_1) \tag{6b}$$

$$\cos(\beta x_2) = \sum_{s=1}^{\infty} h_{ns}\sin(\Psi x_2) \tag{6c}$$

where

$$h_{mr} = \begin{cases} \dfrac{4r}{\pi(r^2 - m^2)}; & m + r = \text{odd};\ m \neq r \\ 0; & m + r = \text{even} \end{cases} \tag{7a}$$

$$h_{ns} = \begin{cases} \dfrac{4s}{\pi(s^2 - n^2)}; & n + s = \text{odd};\ n \neq s \\ 0; & n + s = \text{even} \end{cases} \tag{7b}$$

$$\gamma = \pi r/a, \qquad \Psi = \pi s/b \tag{8}$$

Substituting the series expansions (6) into the first three equations and equating the coefficients of $\sin(\alpha x_1)\sin(\beta x_2)$ on both sides furnishes, after rearrangement, for $x_i \in (0, a)\, x(0, b)$, $i = 1, 2$:

$$\begin{aligned}&[G(i,1)\alpha^2 + G(i,3)\beta^2]U_{mn} + [G(i,4)\alpha^2 + G(i,6)\beta^2]V_{mn} \\ &+ [G(i,7)\alpha^2 + G(i,9)\beta^2]X_{mn} + [G(i,10)\alpha^2 + G(i,12)\beta^2]Y_{mn} \\ &- \sum_{r=1}^{\infty}\sum_{s=1}^{\infty} h_{rm}h_{sn}[G(i,2)U_{rs} + G(i,5)V_{rs} + G(i,8)X_{rs} \\ &+ G(i,11)Y_{rs}]\gamma\Psi = 0; \qquad i = 1, 2\end{aligned} \tag{9a}$$

$$\begin{aligned}&[G(3,1)\alpha^2 + G(3,3)\beta^2]W_{mn} - q_{mn} - \sum_{r=1}^{\infty}\sum_{s=1}^{\infty} h_{rm}h_{sn} \\ &\times G(3,2)\gamma\Psi W_{rs} - \sum_{s=1}^{\infty} h_{sn}G(3,5)X_{ms} + G(3,7)Y_{rn}]\Psi \\ &- \sum_{r=1}^{\infty} h_{rm}[G(3,4)X_{rn} + G(3,6)Y_{rn}]\gamma = 0\end{aligned} \tag{9b}$$

Two more equations are similarly obtained. The above operation finally yields a system of $5mn$ linear algebraic equations in terms of as many unknowns that can be routinely solved, thus providing a boundary-continuous displacement solution to this long-standing practical problem.

Results and Discussion

The following material properties are considered

$$E_1 = 25000 \text{ ksi } (175.78 \text{ GPa}), \qquad \nu_{12} = 0.25$$

$$\frac{E_1}{E_2} = 25, \quad \frac{G_{12}}{E_2} = \frac{G_{13}}{E_2} = 0.5, \quad \frac{G_{23}}{E_2} = 0.2, \quad K = 5/6$$

The normalized displacement and moment quantities are defined as follows:

$$u_i^* = \frac{10^3 E_2 h^2 u_i}{qa^3}; \quad M_i^* = \frac{10^3 M_i}{qa^2} \quad i = 1, 2; \quad u_3^* = \frac{10^3 E_2 h^3 u_3}{qa^4}$$

Numerical results illustrating the convergence of computed normalized central deflection u_3^* and moment M_1^* of a square moderately thick ($a/h = 10$) antisymmetric (45 deg/ − 45 deg) angle-ply plate are presented in Fig. 1. u_3^* exhibits a reasonably rapid, albeit initially oscillatory, convergence, whereas M_1^* displays bounded oscillations. The amplitude of this oscillation, however, decreases with an increase in the number of terms, while the mean value decreases, and the amplitude of oscillation serves as the error norm, in accord with the theory of Fourier series.[4] Figure 2 presents variations with respect to the length-to-thickness ratio a/h of central deflections and moments of square antisymmetric (45 deg/ − 45 deg) and symmetric (45 deg/ − 45 deg)$_s$ angle-ply plates. As expected (see e.g., Ref. 6), the thickness effect, especially in the case of thicker laminates ($a/h \leq 20$), is more pronounced in the computed normalized deflections than in the corresponding moments. Additionally, unlike their classical lamination theory counterparts, these plots do not remain constant with respect to a/h because of inclusion of the effect of transverse shear deformation into the formulation. It is interesting to observe that the normalized deflections of symmetric (45 deg/ − 45 deg)$_s$ angle-ply laminates are lower than their antisymmetric counterparts in the entire range of a/h considered and that the corresponding curves have stiffer slopes, especially in the thicker plate regime, thus bringing the two sets of curves closer in thick plate regime. This suggests, as expected, that the symmetric angle-ply laminates are more shear flexible compared to their antisymmetric counterparts and that the bending-stretching coupling effect that characterizes an antisymmetric laminate compensates to a certain extent the effect of transverse shear deformation. This conclusion is in line with what has been observed in the case of bending of cross-ply plates.[2] The reverse is true, however, in the case of the normalized moments. Variations of the normalized displacements u_3^*, u_1^*, u_2^*, and moments M_1^*, M_2^* of a square moderately thick ($a/h = 10$) general laminate of (0 deg/60 deg) construction, along the centerline parallel to the x_1 axis, are plotted in Figs. 3a and 3b. The normalized deflection u_3^* and moment M_1^*, as

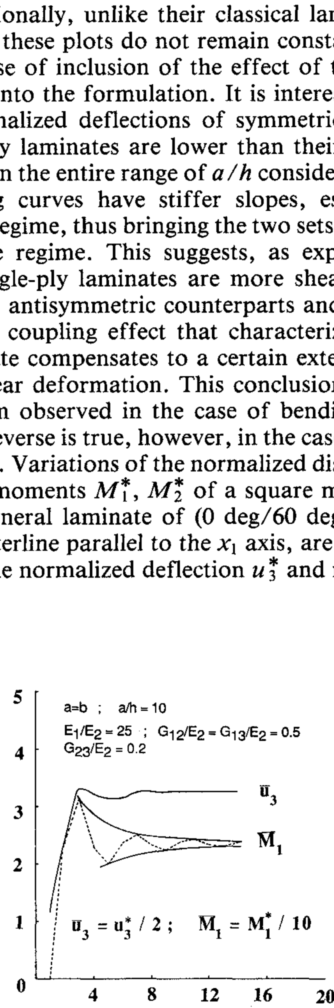

Fig. 1 Convergence of the normalized central deflection and moment of a square moderately thick (a/h = 10) antisymmetric (45 deg/ − 45 deg) angle-ply plate.

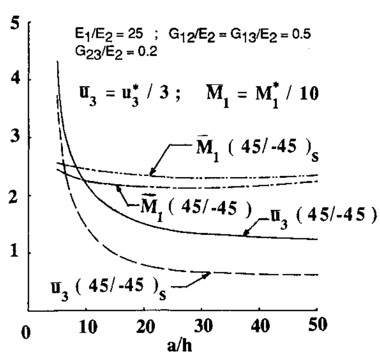

Fig. 2 Variation of the normalized deflections and moments of square antisymmetric (45 deg/ − 45 deg) and symmetric (45 deg/ − 45 deg)$_s$ angle-ply plates with respect to a/h ratio.

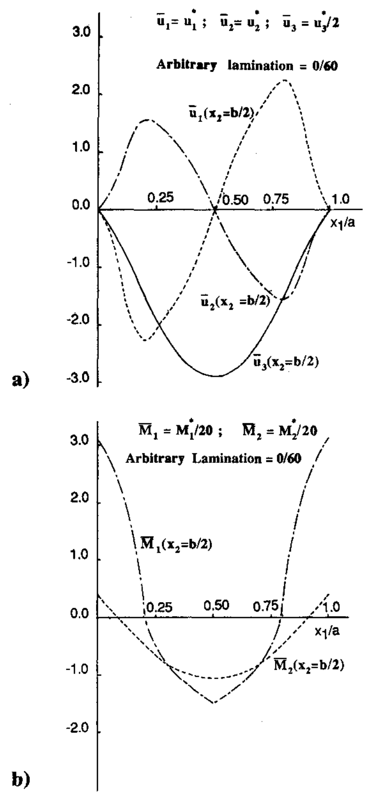

Fig. 3 Variation of the normalized displacements and moments of a square moderately thick ($a/h = 10$) arbitrarily laminated (0 deg/60 deg) plate along the centerline, $x_2 = b/2$: a) displacements; b) moments.

expected, assume their maximum values at the center and edge of the plate, respectively, where in-plane displacements u_1^* and u_2^* vanish. The in-plane displacements u_1^* and u_2^* attain their maximum values near $x_1/a = 0.2$ and 0.8, where M_1^* vanishes. Moment M_2^* attains its maximum magnitude at the center of the plate.

Summary and Conclusions

A novel generalization of the almost two centuries-old Navier's approach is extended to obtain a boundary-continuous-displacement type analytical or strong (differential) form of solution to the hitherto unsolved problem of bending of moderately thick rectangular arbitrarily laminated plates with the rigidly clamped boundary conditions, prescribed at all four edges. The assumed solution functions are in the form of double Fourier sine series, which satisfy the rigidly clamped boundary conditions a priori in a manner similar to Navier's method. The convergence characteristics of the response quantities of interest demonstrate the computational efficiency of the approach. Most interestingly, the bending-stretching type coupling effect has been found to compensate, to a certain extent, the effect of transverse shear deformation. The numerical results presented herein are expected to contribute to achievement of optimal design through composite tailoring.

References

[1]Kabir, H. R. H., and Chaudhuri, R. A., "Boundary Continuous Fourier Solution for Clamped Mindlin Plates," *Journal of the Engineering Mechanics Division, ASCE,* Vol. 118, No. 7, 1992, pp. 1457–1467.

[2]Kabir, H. R. H., and Chaudhuri, R. A., "A Generalized Navier's Approach for Solution of Clamped Moderately Thick Cross-Ply Plates," *Composite Structures,* Vol. 17, No. 4, 1991, pp. 351–366.

[3]Yang, P. C., Norris, C. H., and Stavsky, Y., "Elastic Wave Propagation in Heterogeneous Plates," *International Journal of Solids and Structures,* Vol. 2, No. 4, 1966, pp. 665–684.

[4]Chaudhuri, R. A., "On an Assumed Boundary-Continuous-Displacement Based Fourier Solution to a System of Completely Coupled *n*th Order PDE," unpublished rept.

[5]Green, A. E., and Hearmon, R. F. S., "The Buckling of Flat Rectangular Plywood Plates," *Philosophical Magazine,* Vol. 36, Oct. 1945, pp. 659–687.

[6]Chaudhuri, R. A., and Seide, P., "Triangular Finite Element for Analysis of Thick Laminated Plates," *International Journal for Numerical Methods in Engineering,* Vol. 24, No. 6, 1987, pp. 1203–1224.

Buckling Testing of Composite Columns

Ever Barbero* and John Tomblin†
West Virginia University,
Morgantown, West Virginia 26506

Introduction

THE objective of this Note is to report global (Euler) buckling testing of large composite columns.[1,2] Mass production of composite structural members (e.g., by pultrusion) makes composite materials cost competitive with conventional ones. In the pultrusion process, fibers impregnated with a polymer resin are pulled through a heated die that provides the shape of the cross section to the final product. Pultrusion is a continuous process for manufacturing prismatic sections of virtually any shape,[3] but mainly open or closed thin-walled cross sections. For long composite columns, overall (Euler) buckling is more likely to occur before any other instability failure. For short columns, local buckling occurs first, leading either to large deflections and finally overall buckling, or to material degradation due to large deflections (crippling). The local buckling critical load, determined using a plate analysis,[4] is used in this investigation to limit the long-column region. Because of the large elongation to failure allowed by both the fibers (e.g., 4.8%) and the resin (e.g., 4%), the composite material remains linearly elastic for large deflections and strains, unlike conventional materials that yield (steel) or crack (concrete) for moderate strains. Therefore, buckling is the governing failure for this type of cross section, and the critical buckling load is directly related to the load carrying capacity of the member.

The classical Euler theory[5] used for the buckling of slender columns of isotropic materials reduces the instability problem to a matter of geometry. A similar analysis for pultruded composite columns concludes with the determination of the effective bending stiffness of the cross section, which accounts for the varying material properties. The classical analysis follows Tsai[6] and Vinson[7] but must be complemented by the appropriate plane stress assumption through the width of the beam.[8,9] The material properties of a pultruded column can be accurately predicted from the description of the cross section used in the manufacturing process.[9] Euler's theory assumes an initially straight column with no eccentricity or imperfections, such as initial crookedness. Agreement between the critical load obtained in laboratory experiments and the critical load determined by Euler's analysis is a somewhat fortuitous occurrence and is expected only in the case of perfect columns.

Southwell[10,11] accounted for this inconsistency by using a data reduction technique on the hyperbolic experimental data. In Southwell's method, the critical load is determined by using

Received Nov. 21, 1991; revision received April 27, 1992; accepted for publication April 27, 1992.

*Assistant Professor, Department of Mechanical and Aerospace Engineering.

†Graduate Research Assistant, Department of Mechanical and Aerospace Engineering. Member AIAA.